DISTRIBUTED TURBULENCE MODEL WITH ACCURATE SPATIA CORRELATIONS FOR HELICOPTER HANDLING-QUALITY ANALYSIS

Honglei JI, Renliang CHEN

crlae@nuaa.edu.cn

National Key Laboratory of Science and Technology on Rotorcraft Aeromechanics

Nanjing University of Aeronautics and Astronautics, China

Abstract

This paper presents a distributed turbulence model with the von Karman correlations for helicopter flight simulation and handling-quality analysis. First, turbulence filters based on the longitudinal correlations of the von Karman model are discretized by a high-precision transform method. Turbulence transverse correlations are considered by relating the discrete filters in different positions with spatial correlations of the von Karman model. The distributions of both the related filters on a transverse plane and their velocity components along the longitudinal direction of airspeed are established to form a distributed turbulence model. Then, the turbulence model is integrated into a flight dynamics model and validated against the flight test data. Finally, the effects of both the turbulence filters and turbulence transverse correlations on helicopter handling qualities are discussed. The results show that the Nyquist frequency of sampling period for helicopter flight simulation in atmospheric turbulence should be larger than three times of the interested frequency. The turbulence filters based on the longitudinal correlations of the von Karman model improves the accuracy of helicopter handing-quality analysis in the higher frequency range for the flight conditions with low airspeed and high altitude. The transverse correlations improves the accuracy of helicopter handling-quality analysis in the lower frequency range.

1. INTRODUCTION

Helicopters are always operated at low altitude which is well within the atmospheric boundary layer. The atmospheric turbulence induced by local terrain and man-made structures would result in undesired helicopter motions and high pilot workload, sometimes even push the aircraft to its operational limits. Therefore, it is very critical to develop an atmospheric turbulence model for helicopter safety and handling-quality analysis.

A variety of physics-based turbulence modeling methods, from the traditional body-fixed method for fixed-wing turbulence modeling[1] to the blade-centered and cyclo-stationary random processes[2-4], have been developed to predict helicopter response to atmospheric turbulence. The rotating-frame SORBET (Simulation of Rotor Blade Element Turbulence) model developed by McFarland and Duisenberg[5] is more suitable for helicopter handling-quality analysis due to the favorable assessment obtained in flight simulation and its high computational efficient. It only generated turbulence velocity components at two selected points along an onset line which is perpendicular to the vehicle flight path and tangential to the leading edge of the main rotor. Turbulence velocity components were then distributed with a transport delay in the longitudinal direction and with the Gaussian interpolation method in the lateral direction. One deficiency of the model is “in the reduced level of lateral, longitudinal, and yaw turbulence cues” [5]. Based on the SORBET model, a distributed turbulence model was developed by Ji and Chen[6] to form an atmospheric turbulence field over all the helicopter aerodynamic surfaces. The results of helicopter response to atmospheric turbulence calculated by the distributed model showed a good agreement with the corresponding flight test data. However, both the SORBET and distributed turbulence models were developed based on the Dryden filters, while the more accurate von Karman filters were not used. In addition, both the two models

didn't provide a precise modeling of turbulence transverse correlations. An alternative means of helicopter turbulence modeling is the flight-based Control Equivalent Turbulence Input (CETI) approach[7-9]. It did not generate turbulence velocity directly, but rather generated equivalent control inputs, which produced the same effect on the vehicle as turbulence itself. Due to the extraction from flight test data, the model was automatically validated for specific helicopter type, but the CETI model couldn't be used widely for all the flight conditions and different kinds of helicopters.

This paper presents a distributed turbulence model with the von Karman correlations for helicopter handling-quality analysis. Discrete filters based on the longitudinal correlations of the von Karman model were developed with a high-precision transform method. Turbulence transverse correlations were modeled by relating the discrete filters in different positions with the spatial correlations of the von Karman model. These related filters were placed in front of a helicopter so that their turbulence velocity components could be distributed backward to each of the aerodynamic surfaces as the helicopter was moving forward. Finally, the effects of turbulence filters and transverse correlations on the helicopter handling qualities in turbulent atmospheric environment were discussed.

2. DISTRIBUTED TURBULENCE MODEL WITH VON KARMAN CORRELATIONS

As shown in Fig. 1, the atmospheric turbulence field is represented as a control volume of the cuboid *ABCDEFGH* which covers the whole helicopter and moves together with the helicopter. The front surface *ABCD* sits in front of main rotor and is perpendicular to the airspeed V. The breadth of the rectangle is $2R_{\mathrm{T}}$ and the height is H_{T}, where R_{T} is the radius of main rotor, and H_{T} is dependent on the total height of the helicopter. Related filters with spatial correlations of the von Karman method are placed on the surface *ABCD*. From Taylor's hypothesis[5], the turbulent flow is stationary and homogeneous along the longitudinal direction of airspeed. The outputs of the turbulence filters are statistically valid at either fixed spatial locations or the points translating with the vehicle. In this study, the turbulence velocity components are generated by the related filters with the Gaussian random inputs and are fixed at their inertial positions in the space where they are generated. When the helicopter and cuboid together are moving forward with the airspeed *V*, the turbulence velocity components are distributed backward to each of the helicopter aerodynamic surfaces with a transport delay. The lateral and vertical distributions of the turbulence velocity components over the cuboid volume are achieved with an interpolation method. Thus, a distributed turbulence field is formed for helicopter flight simulation and handling-quality analysis.

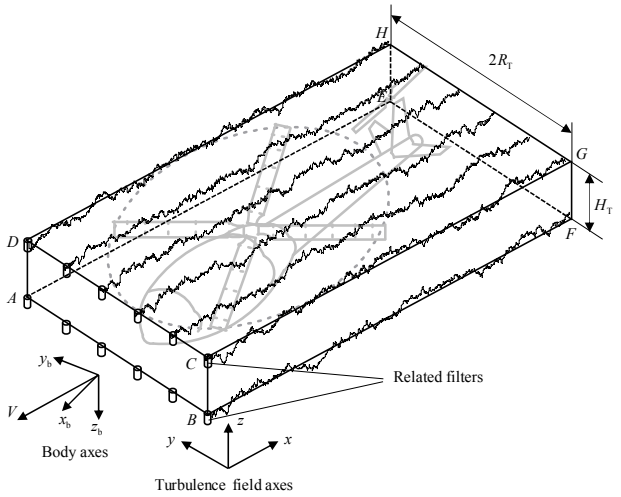

Fig. 1. Distributed turbulence field with related filters.

2.1 Modeling of Unrelated Filters

Firstly, the discrete turbulence filters for generation of independent turbulence velocity components are developed. Based on the longitudinal correlations of the von Karman model, Ji and Chen[10] have developed high-order turbulence filters in the form of transfer functions,

$$(1)\quad H_u(s)=\sigma_u\sqrt{\frac{2}{\pi\gamma_u}}\frac{\left(1+0.25\gamma_u^{-1}s\right)\left(1+0.0244\gamma_u^{-1}s\right)}{\left(1+1.19\gamma_u^{-1}s\right)\left(1+0.167\gamma_u^{-1}s\right)\left(1+0.0170\gamma_u^{-1}s\right)}$$

(2) $$H_v(s)=\sigma_v\sqrt{\frac{1}{\pi\gamma_v}}\frac{\left(1+2.618\gamma_v^{-1}s\right)\left(1+0.12981\gamma_v^{-1}s\right)\left(1+0.0178\gamma_v^{-1}s\right)}{\left(1+2.083\gamma_v^{-1}s\right)\left(1+0.823\gamma_v^{-1}s\right)\left(1+0.08977\gamma_v^{-1}s\right)\left(1+0.0129\gamma_v^{-1}s\right)}$$

(3) $$H_w(s)=\sigma_w\sqrt{\frac{1}{\pi\gamma_w}}\frac{\left(1+2.618\gamma_w^{-1}s\right)\left(1+0.12981\gamma_w^{-1}s\right)\left(1+0.0178\gamma_w^{-1}s\right)}{\left(1+2.083\gamma_w^{-1}s\right)\left(1+0.823\gamma_w^{-1}s\right)\left(1+0.08977\gamma_w^{-1}s\right)\left(1+0.0129\gamma_w^{-1}s\right)}$$

where $\gamma_{u,v,w} = V/L_{u,v,w}$. σ_u , σ_v , and σ_w are the standard deviations of the turbulence velocity components, and L_u , L_v , and L_w are the scale lengths for the turbulence velocity components.

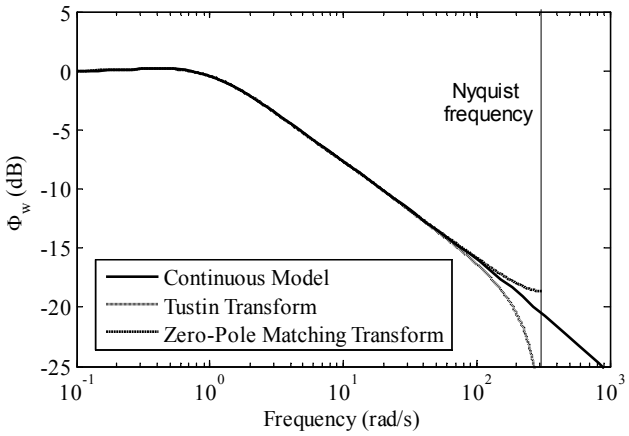

(a) Sampling period Δt =0.01 s

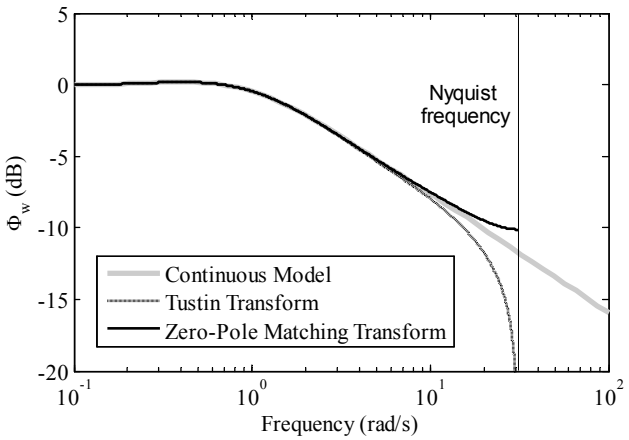

(b) Sampling period Δt =0.1 s

Fig. 2. Comparison between continuous turbulence spectrum and different discrete methods

The Tustin transform has been used for discretization of the turbulence filters[10] because it can simplify the discretization and keep the discrete turbulence filters stable regardless of the sampling period. One deficiency of the Tustin transform is that a great deal of distortion takes place in the frequencies near the Nyquist frequency, as shown in Fig. 2. It can be seen that the discrete spectrum with the Tustin transform matches well with the continuous model in the interested frequency range of handling qualities (1-10 rad/s) as the sampling period is small. However, as the sampling period gets larger, the Nyquist frequency becomes smaller. As a result the disagreement between the continuous and discrete spectra appears in the upper boundary of the interested frequency range. In comparison to the Tustin transform, discretization with the zero-pole matching transform would result in a much less distortion in the frequency range around the Nyquist frequency. Therefore, the zero-pole matching transform are used for discretization of the continuous turbulence filters.

The longitudinal turbulence filter in Eq. (1) can be reorganized as the form

(4) $$H_u(s)=k_u\frac{(s+z_1)(s+z_2)}{(s+p_1)(s+p_2)(s+p_3)}$$

where

$$k_u = 2.5535\sigma_u\sqrt{\gamma_u/\pi}$$
$$\gamma_u = V/L_u$$
$$z_1 = 4\gamma_u$$
$$z_2 = 40.9836\gamma_u$$
$$p_1 = 0.8403\gamma_u$$
$$p_2 = 5.9880\gamma_u$$
$$p_3 = 58.8235\gamma_u$$

Based on the zero-pole matching transform, Eq. (4) can be written as follows by substituting $z=e^{s\Delta t}$ into the equation.

(5) $$H_u(z)=k_u'\frac{\left(z-e^{-z_1\Delta t}\right)\left(z-e^{-z_2\Delta t}\right)}{\left(z-e^{-p_1\Delta t}\right)\left(z-e^{-p_2\Delta t}\right)\left(z-e^{-p_3\Delta t}\right)}$$

where k_u' is solved by matching the gain of $H_u(z)$ with the gain of $H_u(s)$ at the frequency $s=0$, *i.e.*

(6) $$\left|G_u(s)\right|_{s=0}=\left|G_u(z)\right|_{z=1}$$

By solving Eq. (6), k_u' is obtained as

$$(7)\quad k_u' = k_u \frac{z_1 z_2}{p_1 p_2 p_3} \frac{\left(1-e^{-p_1\Delta t}\right)\left(1-e^{-p_2\Delta t}\right)\left(1-e^{-p_3\Delta t}\right)}{\left(1-e^{-z_1\Delta t}\right)\left(1-e^{-z_2\Delta t}\right)}$$

By inspecting Eq. (7) with zero initial conditions[11], we can obtain the difference equations for the longitudinal velocity component

$$(8)\quad \begin{aligned} y_{n+3} = {} & f_{y2} y_{n+2} + f_{y1} y_{n+1} + f_{y0} y_n + \\ & k_u' \left(x_{n+2} + f_{x1} x_{n+1} + f_{x0} x_n\right) \end{aligned}$$

where x_n and y_n represent the discrete Gaussian white noise input and longitudinal turbulence velocity component output of the difference equations at the time $t = n\Delta t$. The coefficients in Eq. (8) are,

$$\begin{aligned} f_{y2} &= e^{-p_1\Delta t} + e^{-p_2\Delta t} + e^{-p_3\Delta t} \\ f_{y1} &= -e^{-(p_1+p_2)\Delta t} - e^{-(p_1+p_3)\Delta t} - e^{-(p_2+p_3)\Delta t} \\ f_{y0} &= e^{-(p_1+p_2+p_3)\Delta t} \\ f_{x1} &= -e^{-z_1\Delta t} - e^{-z_2\Delta t} \\ f_{x0} &= e^{-(z_1+z_2)\Delta t} \end{aligned}$$

Generally, the generated discrete Gaussian white noise is measured with the spectrum of unit strength other than unit power. The above Gaussian white noise will reduce the spectrum of the turbulence velocity components by $\Delta t/\pi$. This effect can be removed by multiplying the coefficients of the random input in Eq. (8) with $\sqrt{\Delta t/\pi}$. Therefore, the coefficient k_u' of the random input is corrected as,

$$\begin{aligned} k_u' = {} & 2.5535\sigma_u \sqrt{\gamma_u/\Delta t} \cdot \\ & \frac{z_1 z_2}{p_1 p_2 p_3} \frac{\left(1-e^{-p_1\Delta t}\right)\left(1-e^{-p_2\Delta t}\right)\left(1-e^{-p_3\Delta t}\right)}{\left(1-e^{-z_1\Delta t}\right)\left(1-e^{-z_2\Delta t}\right)} \end{aligned}$$

For the lateral and vertical turbulence filters, they can be reorganized as the form

$$(9)\quad H_{v,w}(s) = k_{v,w} \frac{(s+z_1)(s+z_2)(s+z_3)}{(s+p_1)(s+p_2)(s+p_3)(s+p_4)}$$

where

$$\begin{aligned} k_{v,w} &= 3.0471\sigma_{v,w}\sqrt{\gamma_{v,w}/\pi} \\ \gamma_{v,w} &= V/L_{v,w} \\ z_1 &= 0.3820\gamma_{v,w} \\ z_2 &= 7.7036\gamma_{v,w} \\ z_3 &= 56.1798\gamma_{v,w} \\ p_1 &= 0.4801\gamma_{v,w} \\ p_2 &= 1.2151\gamma_{v,w} \\ p_3 &= 11.1396\gamma_{v,w} \\ p_4 &= 77.5194\gamma_{v,w} \end{aligned}$$

A similar approach for the longitudinal turbulence filter can be taken for the reorganized filters in Eq. (9). The resulting difference equations are

$$(10)\quad \begin{aligned} y_{n+4} = {} & g_{y3} y_{n+3} + g_{y2} y_{n+2} + g_{y1} y_{n+1} + g_{y0} y_n + \\ & k_{v,w}' \left(x_{n+3} + g_{x2} x_{n+2} + g_{x1} x_{n+1} + g_{x0} x_n\right) \end{aligned}$$

where y_n represents the discrete lateral or vertical turbulence velocity component output of the difference equations at the time $t = n\Delta t$. The coefficients for the lateral and vertical case are,

$$\begin{aligned} k_{v,w}' = {} & 3.0471\sigma_{v,w}\sqrt{\gamma_{v,w}/\Delta t} \cdot \frac{z_1 z_2 z_3}{p_1 p_2 p_3 p_4} \cdot \\ & \frac{\left(1-e^{-p_1\Delta t}\right)\left(1-e^{-p_2\Delta t}\right)\left(1-e^{-p_3\Delta t}\right)\left(1-e^{-p_4\Delta t}\right)}{\left(1-e^{-z_1\Delta t}\right)\left(1-e^{-z_2\Delta t}\right)\left(1-e^{-z_3\Delta t}\right)} \\ g_{y3} = {} & e^{-p_1\Delta t} + e^{-p_2\Delta t} + e^{-p_3\Delta t} + e^{-p_4\Delta t} \\ g_{y2} = {} & -e^{-(p_1+p_2)\Delta t} - e^{-(p_1+p_3)\Delta t} - e^{-(p_1+p_4)\Delta t} - \\ & e^{-(p_2+p_3)\Delta t} - e^{-(p_2+p_4)\Delta t} - e^{-(p_3+p_4)\Delta t} \\ g_{y1} = {} & e^{-(p_1+p_2+p_3)\Delta t} + e^{-(p_1+p_2+p_4)\Delta t} + e^{-(p_1+p_3+p_4)\Delta t} + \\ & e^{-(p_2+p_3+p_4)\Delta t} \\ g_{y0} = {} & -e^{-(p_1+p_2+p_3+p_4)\Delta t} \\ g_{x2} = {} & -e^{-z_1\Delta t} - e^{-z_2\Delta t} - e^{-z_3\Delta t} \\ g_{x1} = {} & e^{-(z_1+z_2)\Delta t} + e^{-(z_1+z_3)\Delta t} + e^{-(z_2+z_3)\Delta t} \\ g_{x0} = {} & -e^{-(z_1+z_2+z_3)\Delta t} \end{aligned}$$

2. 2 Modeling of Related Filters

The total number of the related filters arranged on the plane *ABCD* is assumed to be N. These N sets of independent vertical turbulence velocity sequences with zero mean value and the same standard deviation σ_w can be generated by Eq. (10), which are denoted as $\{\Delta w^1\}, \{\Delta w^2\}, \cdots, \{\Delta w^N\}$. Here the vertical turbulence velocity component is taken as an example to show how to relate the independent turbulence velocity component sequences for the formation of related filters. Based on the von Karman model[12], the spatial correlations between the dependent vertical turbulence velocity sequences

$\{\Delta W^1\},\{\Delta W^2\},\cdots,\{\Delta W^N\}$ of the N related filters on the plane *ABCD* have the form,

$$(11)\quad R_{WW}(i,j)=\frac{2^{2/3}}{\Gamma(1/3)}\zeta^{1/3}\left\{K_{1/3}(\zeta)-K_{2/3}(\zeta)\frac{\xi_2^2+\xi_1^3}{2aL_w\xi}\right\}$$

where $\xi_1=|x_i-x_j|$, $\xi_2=|y_i-y_j|$, $\xi_3=|z_i-z_j|$, $\xi=\sqrt{\xi_1^2+\xi_2^2+\xi_3^2}$, $\zeta=\xi/(aL_w)$, and a =1.339. x_i, y_i,z_i and x_j,y_j,z_j are the coordinates of the i th and j th filters on the plane *ABCD*, Γ is the gamma function, and K is the modified Bessel function of second kind.

The correlation coefficient matrix $\boldsymbol{R_{WW}}=\left[R_{WW}(i,j)\right]$ between the vertical turbulence components of the related filters in different spatial positions can be obtained with Eq. (11). Since the correlation coefficient matrix is positive and symmetric, a lower triangular matrix $\boldsymbol{A}$ can be produced with the Cholesky decomposition[13] of the matrix $\boldsymbol{R_{WW}}$, which satisfies the equation

$$(12)\quad \boldsymbol{R_{WW}}=\boldsymbol{A}\boldsymbol{A}^T$$

with

$$\boldsymbol{A}=\begin{bmatrix} a_{11} & 0 & \cdots & 0\\ a_{21} & a_{22} & \cdots & 0\\ \vdots & \vdots & \ddots & \vdots\\ a_{N1} & a_{N2} & \cdots & a_{NN}\end{bmatrix}$$

The dependent turbulence velocity sequences $\{\Delta W^1\},\{\Delta W^2\},\cdots,\{\Delta W^N\}$, can be obtained by relating the independent sequences with a transformation as follows,

$$(13)\quad \Delta\boldsymbol{W}=\boldsymbol{A}\Delta\boldsymbol{W}$$

where $\Delta\boldsymbol{W}=\left(\Delta W^1,\Delta W^2,\cdots,\Delta W^N\right)^T$ and $\Delta\boldsymbol{w}=\left(\Delta w^1,\Delta w^2,\cdots,\Delta w^N\right)^{\mathrm{T}}$.

It can be proven that the turbulence velocity sequences $\{\Delta W^1\}$, $\{\Delta W^2\},\cdots,\{\Delta W^N\}$ have a correlation coefficient matrix $\boldsymbol{R_{WW}}$. Since $E\left(\Delta w^i\Delta w^j\right)=\delta_{ij}\sigma_w^2$, where δ_{ij} is the Kronecker delta, the expected values for the dependent variables are given by

$$(14)\quad \begin{aligned}E\left(\Delta W^i\Delta W^j\right)&=E\left\langle\left(\sum_{k=1}^{i}a_{ik}\Delta w_k\right)\cdot\left(\sum_{k=1}^{j}a_{jk}\Delta w_k\right)\right\rangle\\&=\sum_{k=1}^{\min(i,j)}a_{ik}a_{jk}E\left[\left(\Delta w^k\right)^2\right]=\sigma_w^2\sum_{k=1}^{\min(i,j)}a_{ik}a_{jk}\end{aligned}$$

With Eq. (12) we have

$$(15)\quad \sum_{k=1}^{\min(i,j)}a_{ik}a_{jk}=R_{WW}(i,j)$$

Substitute Eq. (15) in to Eq. (14), we obtain

$$(16)\quad E\left(\Delta W^i\Delta W^j\right)=\sigma_w^2R_{WW}(i,j)$$

Therefore, the correlation coefficient $R'_{WW}(i,j)$ between the vertical turbulence velocity sequences $\{\Delta W^i\}$ and $\{\Delta W^j\}$ is

$$(17)\quad E\left(\Delta W^i\Delta W^j\right)=\sigma_w^2R_{WW}(i,j)$$

It is easy to see that the dependent turbulence velocity sequences $\{\Delta W^1\}$, $\{\Delta W^2\},\cdots,\{\Delta W^N\}$ have a correlation coefficient matrix $\boldsymbol{R_{WW}}$.

With the preceding method, the dependent longitudinal and lateral turbulence velocity sequences of the related filters with zero mean values and the same standard deviations σ_u and σ_v can be generated. The related filters with spatial correlations of the von Karman model can be formed.

2. 3 Filter Distribution on the Transverse Plane

The related filters are distributed to cover the whole plane *ABCD* with the same equal interval in the lateral and vertical directions. In this study, the interval is chosen to make the correlation coefficients between the vertical turbulence velocity components of the adjacent filters larger than 0.95. Thus, the interval Δd_{f} is determined by the scale length for the vertical turbulence spectrum[1],

$$(18)\quad \Delta d_{\mathrm{f}}=0.02L_{\mathrm{w}}$$

With the interval Δd_{f}, the numbers of the filters in each row and column on the plane *ABCD*, m_{f} and n_{f}, are determined,

$$(19)\quad m_{\mathrm{f}}=\left\lfloor\frac{2R_{\mathrm{T}}}{\Delta d_{\mathrm{f}}}\right\rfloor+1$$

(20) $n_{\mathrm{f}} = \left\lceil \frac{H_{\mathrm{T}}}{\Delta d_{\mathrm{f}}} \right\rceil + 1$

where "⌈ ⌉" denotes the integer ceiling operator.

The vertical turbulence scale length decreases with the decrement of flight altitude[1]. From Eqs. (19) and (20) it can be obtained that the total numbers of the filters arranged on the plane *ABCD* would increase with the decrement of flight altitude. However, large numbers of filters would reduce the computational efficiency. Since the distribution of the aircraft aerodynamic surfaces in the lateral and vertical directions of the turbulence field is not so close, intensive arrangement of the filters is not necessary. The maximum numbers of the filters in each row and column on the plane *ABCD*, m_{fmax} and n_{fmax}, are selected depending on the distribution of the aircraft aerodynamic surfaces,

(21) $m_{\mathrm{f}} = \begin{cases} m_{\mathrm{f}}, & if\ m_{\mathrm{f}} \le m_{\mathrm{fmax}} \\ m_{\mathrm{fmax}}, & if\ m_{\mathrm{f}} > m_{\mathrm{fmax}} \end{cases}$

(22) $n_{\mathrm{f}} = \begin{cases} n_{\mathrm{f}}, & if\ n \le n_{\mathrm{fmax}} \\ n_{\mathrm{fmax}}, & if\ n > n_{\mathrm{fmax}} \end{cases}$

2. 4 Turbulence Distribution in Longitudinal Direction

When the helicopter and cuboid together are moving forward with the airspeed V and computing cycle Δt, the turbulence velocity components are distributed backward to cover each of the helicopter aerodynamic surfaces with a transport delay, as shown in Fig. 1. If the turbulence field is divided into a rectangle grid, which has ($l_{\mathrm{g}} \times m_{\mathrm{f}} \times n_{\mathrm{f}}$) grid points with the equal interval $\Delta d = V\Delta t$ in the longitudinal direction of airspeed and Δd_{f} in the lateral and vertical directions, the discrete turbulence velocity components will always be located at the grid points, and move to next grid points at next computing cycle. Meanwhile the tables $U_{j,k}(l_{\mathrm{g}})$, $V_{j,k}(l_{\mathrm{g}})$, and $W_{j,k}(l_{\mathrm{g}})$ (j = 1, 2, …, m_{f}, k = 1, 2, …, n_{f}, and l_{g} is the size of the tables) are created to store the turbulence velocity components generated by the filter in the j th column and kth row on the plane ABCD in reverse order from their last elements to the first circularly. That is, if the turbulence velocity components generated by the filters at the last computing cycle are stored in the ith elements of the circular tables, the newly generated turbulence velocity components will be stored in the (*i*-1)th elements. When the tables are filled fully as the simulation goes by, the newly generated data of the turbulence velocity components will refresh the tables from their last elements again. There exists a one-to-one mapping relationship between the grid points of the turbulence field in Fig. 3 and the turbulence velocity components stored in the tables. At the time $t = n\Delta t$, the latest turbulence velocity components are supposed to be stored in the (l_0 +1)th elements of the tables, with

(23) $l_0 = l_g - n\%l_g$

where "%" denotes the modulo operator. Then the turbulence velocity components at the grid point (i, j, k) are $U_{j,k}(l)$, $V_{j,k}(l)$, and $W_{j,k}(l)$, with

(24) $l = \begin{cases} l_0 + i, & if\quad l_0 + i \le l_g \\ l_0 + i - l_g, & if\quad l_0 + i > l_g \end{cases}$

For each point which is not located at the grid points, the turbulence velocity components can be regarded to be the same as those of the nearest grid point. Furthermore, the turbulence velocity components generated by the related filters are assumed to be constant over each computing cycle. Therefore, with the coordinates (x, y, z) of the inquired point in the turbulence field, the turbulence velocity components at the time $t = n\Delta t$ can be determined as $U_{j,k}(l)$, $V_{j,k}(l)$, and $W_{j,k}(l)$, with

(25) $l = \begin{cases} l_0 + i, & if\quad l_0 + i \le l_g \\ l_0 + i - l_g, & if\quad l_0 + i > l_g \end{cases}$

(26) $l = \begin{cases} l_0 + i, & if\quad l_0 + i \le l_g \\ l_0 + i - l_g, & if\quad l_0 + i > l_g \end{cases}$

and

(27) $j = \left\lfloor \frac{y_{i,j}}{\Delta d_f} + 0.5 \right\rfloor$

(28) $k = \left\lfloor \frac{z_{i,j}}{\Delta d_f} + 0.5 \right\rfloor$

where "$\lfloor\ \rfloor$" denotes the integer floor operator.

Once the table size l_g is established for storing the discrete turbulence velocity components, the minimum airspeed $V_{\min}$ for the turbulence filters is determined by distributing the table elements over each of the helicopter aerodynamic surfaces, that is

(29) $l_g V_{\min} \Delta t = L_T$

where L_T is the total helicopter length. To make the tables always cover the whole helicopter, the flight speed V_{tb} for the turbulence filters must be always larger than the minimum airspeed $V_{\min}$,

(30) $V_{\text{tb}} = \begin{cases} V & V \geq V_{\min} \\ V_{\min} & V < V_{\min} \end{cases}$

With the above method, the discrete turbulence velocity components generated by the related filters are distributed to the turbulence field.

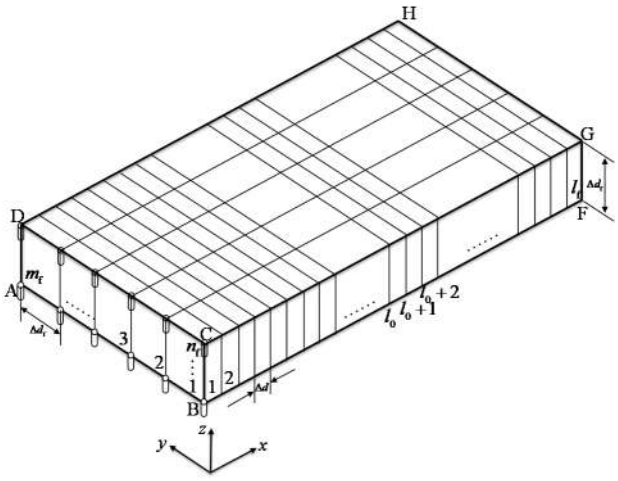

Fig. 3. Turbulence field divided by rectangle grid.

2.5 Validation of Distributed Turbulence Model

The spectra and correlation coefficients of the simulated turbulence velocity components by the distributed turbulence model are calculated and compared to those of the theoretical von Karman model. The flight condition here is the case for a helicopter hovering at the altitude of 12.2 m with the mean wind speed of 11.3 m/s and the vertical turbulence intensity of 1.68 m/s. There are 40 filters arranged in 2 rows on the whole plane *ABCD* with 20 filters in each row for this flight condition.

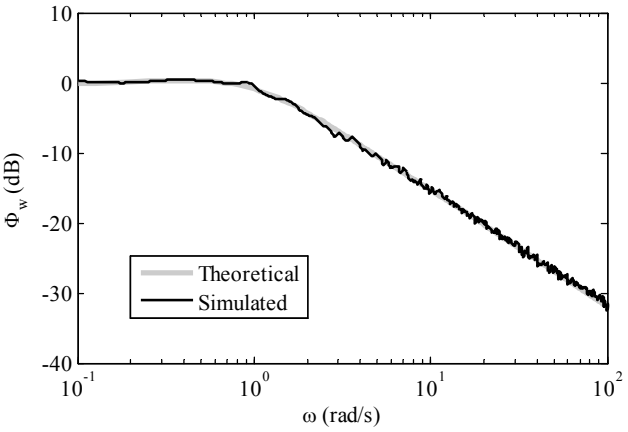

(a) Sampling period Δt =0.01 s

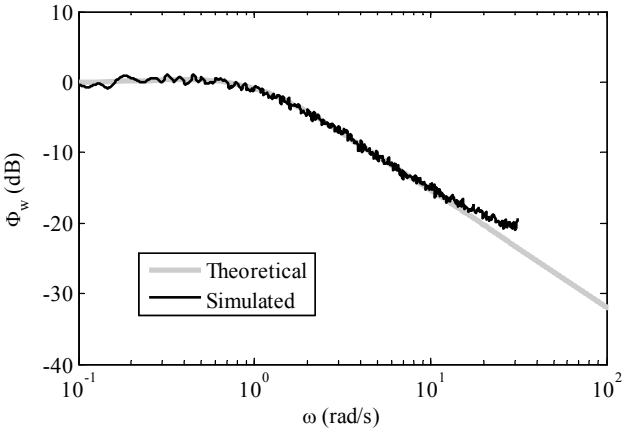

(b) Sampling period Δt =0.1 s

Fig. 4. Comparison between theoretical and calculated spectra of vertical turbulence velocity components with different sampling periods.

Fig. 4 shows the comparison between the theoretical and calculated spectra of the vertical turbulence velocity components generated by the related filters with different sampling periods. We can see that even for the case with a sampling period of 0.1 s the spectrum of the simulated vertical turbulence velocity component matches well with the theoretical von Karman spectrum in the interested frequency range of handling qualities. For a reasonable analysis of helicopter handling qualities in turbulence, it is suggested that the Nyquist frequency of the sampling period is larger than three times of the interested frequency.

Fig. 5 presents the comparison between the theoretical and calculated correlation coefficients of the vertical turbulence velocity components from the 20 filters in the upper row. It can be seen that the agreement between the theoretical and simulated correlation coefficients of the related filters is quite satisfactory for handling-quality analysis. The calculated correlation coefficients of the longitudinal and lateral turbulence velocity components have the same accuracy.

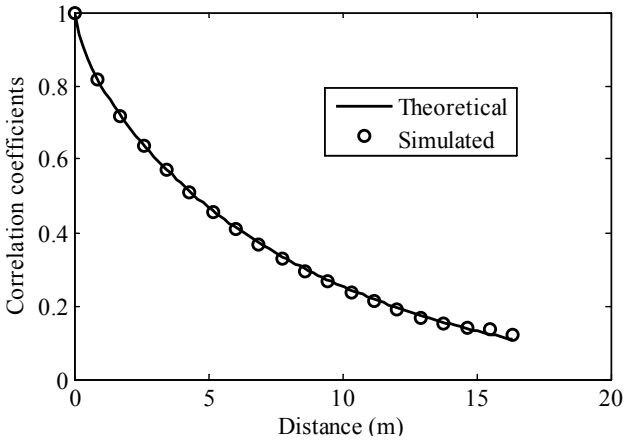

Fig. 5. Comparison between theoretical with calculated correlation coefficients of vertical turbulence velocity components.

3. SIMULATION MODEL FOR HELICOPTER FLIGHT IN ATMOSPHERIC TURBULENCE

3. 1 Turbulence Models on Helicopter Aerodynamic Surfaces

The turbulence velocity components on each blade element of main rotor are presented firstly. Due to the rotation of blades, the position of a blade element in the turbulence field varies with time. For the sake of reducing the amount of computations, the flapping motions of main rotor blades are assumed to be small and the tip path plane of main rotor located on the upper surface *DCGH* of the turbulence field. As shown in Fig. 6, the azimuth angle of the blade i at the time t is given by

$$\psi_i = \int \Omega_T dt + 2\pi\left(\frac{i-1}{N_b}\right) \quad (31)$$

where $2\pi(i-1)/N_b$ is the initial azimuth angle of the blade *i*.

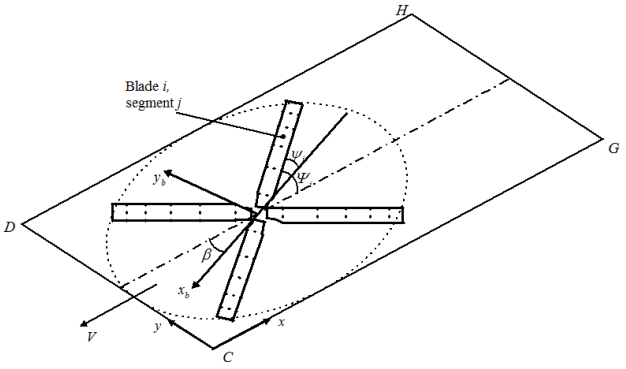

Fig. 6. Coordinates of main rotor blade elements.

Helicopter airspeed is not always parallel to the longitudinal body axis, as shown in Fig. 6. The sideslip angle is,

$$\beta = \arctan\left(\frac{v}{u}\right) \quad (32)$$

where *u* and v are the horizontal components of the flight speed V in body axes. Thus the aerodynamic azimuth angle in wind axes is,

$$\Psi_i = \psi_i + \beta \quad (33)$$

Considering the main rotor hinge offset and lag angle, the coordinates of the blade i element j on the surface DCGH are

$$\begin{aligned} x_{i,j} &= R + e\cos\Psi_i + r_j\cos\left(\Psi_i + \varsigma_i\right) \\ y_{i,j} &= R + e\sin\Psi_i + r_j\sin\left(\Psi_i + \varsigma_i\right) \end{aligned} \quad (34)$$

where e is the main rotor hinge offset, r_j is the radial station of the blade i element j, and ς_i is the lag angle of the blade i.

With the coordinates of the blade element in the turbulence field, the turbulence velocity components can be obtained with Eqs. (23) and (25)-(28).

The models for the turbulence velocity components of fuselage, horizontal stabilator, vertical fin, and tail rotor are alike. In order to determine the turbulence velocity components at the center pressure of the helicopter aerodynamic surfaces, their coordinates in the turbulence field should be obtained with helicopter geometry parameters and flight states in advance. Then the turbulence velocity components can be obtained with Eqs. (23) and (25)-(28).

3.2 Flight Dynamics Model Coupled with Turbulence Model

A high-order nonlinear helicopter flight dynamics model is used for flight simulation. The detailed formulation and validation of the mathematical model can be obtained in Refs. [6], [14], and [15] respectively. The impact of the atmospheric turbulence on helicopter is considered by adding the turbulence velocity components of the helicopter aerodynamic surfaces (including main rotor, fuselage, horizontal stabilator, vertical fin, and tail rotor) directly to the relative incidence velocity components of each surface. For the UH-60 helicopter with a main rotor of four blades, the state-space form of the model is shown as follows

(35) $\dot{\boldsymbol{x}} = f\left(\boldsymbol{x},\boldsymbol{u},\boldsymbol{w},t\right)$

where $\boldsymbol{x}$ is the aircraft state vector,

(36) $$\boldsymbol{x}=\begin{bmatrix} u\,v\,w\,p\,q\,r\,\Phi\,\Theta\,\Psi\,\dot{\beta}_1\,\dot{\beta}_2\,\dot{\beta}_3\,\dot{\beta}_4\,\beta_1\,\beta_2\,\beta_3\,\beta_4\,\dot{\varsigma}_1\,\dot{\varsigma}_2\,\dot{\varsigma}_3\,\dot{\varsigma}_4 \\ \varsigma_1\,\varsigma_2\,\varsigma_3\,\varsigma_4\,\phi_1\,\phi_2\,v_0\,v_{\mathrm{c}}\,v_{\mathrm{s}}\,v_{\mathrm{tr}}\,v_{\mathrm{x}}\,v_{\mathrm{y}} \end{bmatrix}^T$$

u,v,w,p,q,r are the aircraft translational velocity components and angular rates, Φ,Θ,Ψ are the aircraft Euler angles, $\dot{\beta}_1,\dot{\beta}_2,\dot{\beta}_3,\dot{\beta}_4$, $\beta_1,\beta_2,\beta_3,\beta_4$ are the flap angular rates and angles of the four rigid blades, $\dot{\varsigma}_1,\dot{\varsigma}_2,\dot{\varsigma}_3,\dot{\varsigma}_4$, $\varsigma_1,\varsigma_2,\varsigma_3,\varsigma_4$ are the lag angular rates and angles of the four rigid blades, ϕ_1,ϕ_2 are the blade tip dynamic torsion states, $v_0,v_{\mathrm{c}},v_{\mathrm{s}}$ are the induced velocity components of main rotor, v_{tr} is the induced velocity component of tail rotor, and $v_{\mathrm{x}},v_{\mathrm{y}}$ are the delayed fuselage downwash and sidewash. $\boldsymbol{u}$ is the control vector,

(37) $$\boldsymbol{u}=\begin{bmatrix}\delta_{\mathrm{col}}\,\delta_{\mathrm{lat}}\,\delta_{\mathrm{lon}}\,\delta_{\mathrm{ped}}\end{bmatrix}^T$$

where δ_{col} is the collective stick input, δ_{lat} is the lateral stick input, δ_{lon} is the longitudinal stick input, and δ_{ped} is the pedal input. $\boldsymbol{w}$ is the turbulence velocity vector of the helicopter aerodynamic surfaces,

(38) $$\boldsymbol{w}=\begin{bmatrix}\Delta U_{i,j}\,\Delta V_{i,j}\,\Delta W_{i,j}\,\Delta U_{\mathrm{wf}}\,\Delta V_{\mathrm{wf}}\,\Delta W_{\mathrm{wf}}\,\Delta U_{\mathrm{hs}}\,\Delta V_{\mathrm{hs}}\,\Delta W_{\mathrm{hs}} \\ \Delta U_{\mathrm{vt}}\,\Delta V_{\mathrm{vt}}\,\Delta W_{\mathrm{vt}}\,\Delta U_{\mathrm{tr}}\,\Delta V_{\mathrm{tr}}\,\Delta W_{\mathrm{tr}}\end{bmatrix}^{\mathrm{T}}$$

where $\Delta U_{i,j},\Delta V_{i,j},\Delta W_{i,j}$ are the turbulence velocity components of main rotor blade elements, $\Delta U_{\mathrm{wf}},\Delta V_{\mathrm{wf}},\Delta W_{\mathrm{wf}}$ are the turbulence velocity components of fuselage, $\Delta U_{\mathrm{hs}},\Delta V_{\mathrm{hs}},\Delta W_{\mathrm{hs}}$ are the turbulence velocity components of horizontal stabilator, $\Delta U_{\mathrm{vt}},\Delta V_{\mathrm{vt}},\Delta W_{\mathrm{vt}}$ are the turbulence velocity components of vertical fin, and $\Delta U_{\mathrm{tr}},\Delta V_{\mathrm{tr}},\Delta W_{\mathrm{tr}}$ are the turbulence velocity components of tail rotor. The subscripts i,j indicate that the argument is the turbulence velocity component of the blade *i* element *j*. *t* represents time.

3.3 Pilot Model

A simplified precision model of pilot[16] is used to consider the influence of pilot's control behavior on the frequency response to atmospheric turbulence. The pilot model can be described by the transfer function

(39) $$Y_{\mathrm{P}}\left(s\right)=K_{\mathrm{P}}\frac{T_{\mathrm{L}}s+1}{T_{\mathrm{D}}s+1}\frac{e^{-\tau s}}{T_{\mathrm{N}}s+1}$$

where K_{P} is the pilot gain representing the pilot's ability to respond to an error in the magnitude of a controlled variable, T_{L} is the lead time constant reflecting the pilot's ability to predict a control input and T_{D} is the lag time constant which describes the ease with which the pilot generates the required input. $e^{-\tau s}$ represents a pure time delay to model pilot's cognitive responsiveness. T_{N} is the neuromuscular lag time constant which represents the time constant associated with contraction of the muscles through which the control input is applied by the pilot.

3.4 Validation of Simulation Model

The simulation model for helicopter flight in atmospheric turbulence is validated by comparing the simulated helicopter response to turbulence to the flight test data in Ref. [8] of the Power Spectral Densities (PSD) for the roll, pitch, yaw, and heave rates. The flight condition is the case for a helicopter hovering at the altitude of 12.2 m with the mean wind speed of 11.3 m/s and the vertical turbulence intensity of 1.68 m/s. The results are shown in Fig. 7.

From the figure it can be seen that the simulated helicopter angular and heave responses to turbulence by the proposed distributed turbulence

model with the von Karman correlations are in good agreement with those from flight test in the interested frequency range of 1-10 rad/s.

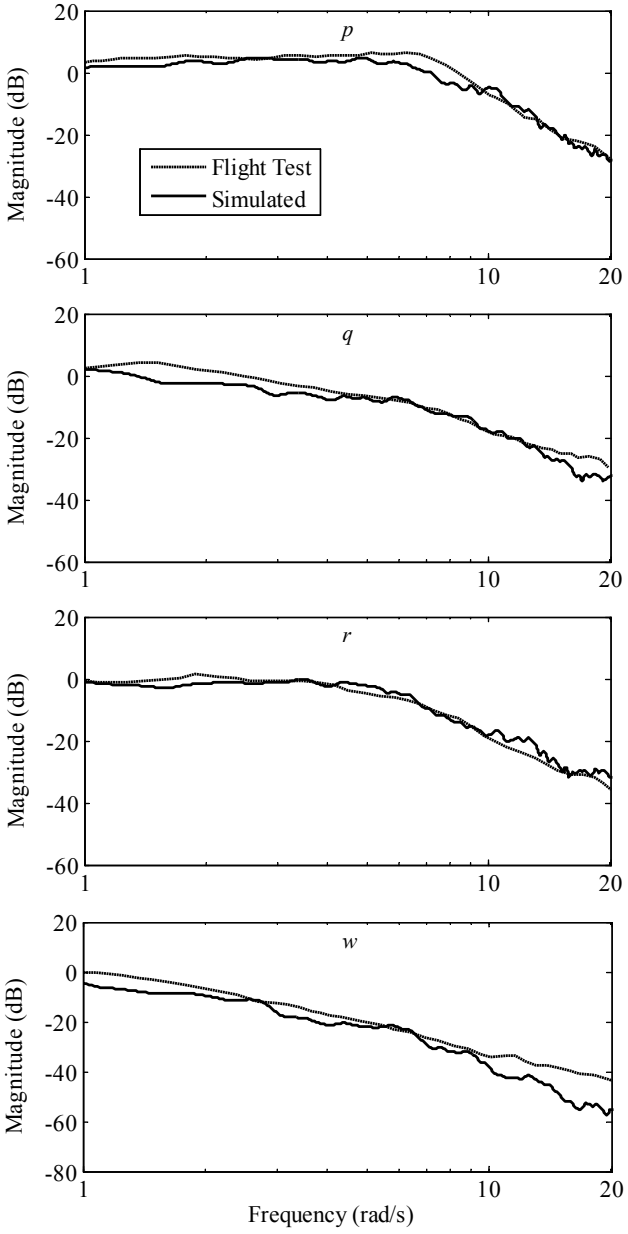

Fig. 7. Comparison between simulated helicopter response to turbulence and flight test data.

4. EFFECTS OF TURBULENCE CORRELATIONS ON HELICOPTER HANDLING QUALITIES

Smith[19] proposed that, in any closed-loop tracking task such as attitude regulation in atmospheric turbulence, rate control activity is of fundamental importance from the standpoint of pilot controlling and perceiving vehicle handling qualities. Based on Smith's fundamental idea, the impact of turbulence longitudinal and transverse correlations on helicopter handling qualities can be analyzed by comparing the helicopter angular and heave rate responses to turbulence with different correlations.

4. 1 Effect of Turbulence Longitudinal Correlations on Helicopter Handling Qualities

In comparison to the turbulence filters based on the longitudinal correlations of the von Karman model, those based on the longitudinal correlations of the Dryden model have been used widely in the current turbulence models[2, 3, 5, 6] for helicopter handling-quality analysis. In this section, the helicopter responses to turbulence by the von Karman and Dryden filters are compared to show the effect of turbulence longitudinal correlations on helicopter handling qualities.

Fig. 8 shows the comparison of roll rate response to turbulence by the Dryden and von Karman filters respectively. For the case with γ_w =1, the flight condition is for a helicopter flying at the altitude of 10 m with the speed of 10 m/s as well as the vertical turbulence intensity of 1.5 m/s, while for the case with γ_w =0.2, the flight condition is for a helicopter flying at the altitude of 50 m with the speed of 10 m/s as well as the vertical turbulence intensity of 2.5 m/s. The derivation of the discrete Dryden filters can be obtained in Ref. [6].

From the figure it can be seen that for the case with γ_w =1, the helicopter response to turbulence by the von Karman filters is a little larger than that by the Dryden filters only in the higher frequency range of handling qualities. However, for the case with γ_w =0.2, the difference becomes greater and spreads into the lower frequencies. This is because that the valid normalized frequency range of the Dryden filters is only up to 10 rad[10]. For the flight conditions with $\gamma_w \geq 1$ both the von Karman and Dryden filters are valid in the interested frequency range of 1-10 rad/s, while for the latter case with $\gamma_w < 1$ only the von Karman filters is valid in the interested frequency range. Since the turbulence scale lengths increase with flight altitude[1], the turbulence filters based on

the longitudinal correlations of the von Karman model improve the accuracy of the handling-quality analysis in the higher frequency range for the flight conditions with low airspeed and high altitude.

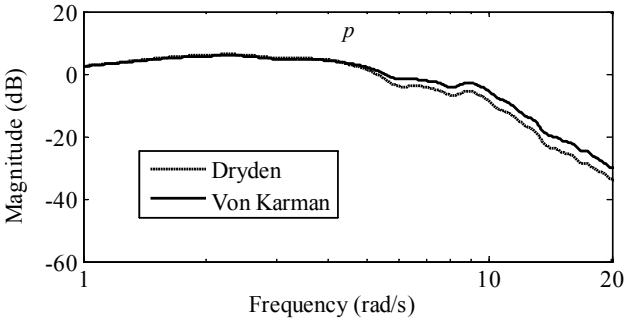

(a) γ_w =1

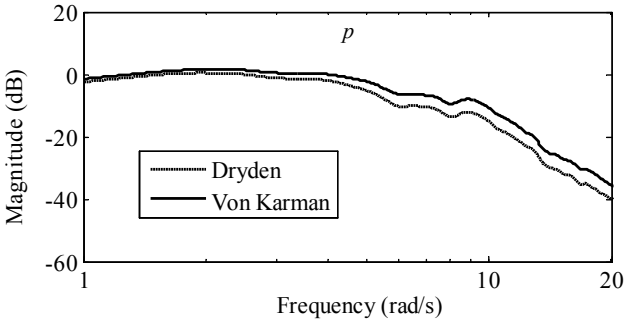

(b) γ_w =0.2

Fig. 8. Comparison of roll rate response to turbulence by Dryden and von Karman filters.

4. 2 Effect of Turbulence Transverse Correlations on Helicopter Handling Qualities

The effect of turbulence transverse correlations on helicopter handling qualities are analyzed by comparing helicopter response to turbulence with and without transverse correlations. Turbulence with transverse correlations are modeled by the related filters, while that without transverse correlations are modeled by the unrelated filters.

Fig. 9 shows the comparison of helicopter angular and heave rate frequency responses to atmospheric turbulence between the cases by the unrelated and related filters respectively. The flight condition is the case for a helicopter hovering at the altitude of 12.2 m with the mean wind speed of 11.3 m/s and the vertical turbulence intensity of 1.68 m/s. From the figure we can find that neglect of the transverse correlations only results in great underestimate of the roll and heave rate responses to turbulence in the lower interested frequency range, results in a little underestimate of the pitch rate response, but nearly has no effect on the yaw rate response. The reason is that in comparison to the case with the related filters, the excessive randomness of the turbulence disturbances over the main rotor in the case with the unrelated filters aggravates the “rotor-to-body attenuation” effect[5], which indicates that much energy is lost as the turbulence disturbances over the main rotor are transferred to body due to the randomness of the blade element turbulence velocity components. Meanwhile, although the main rotor has dominant effects on both the roll and heave rate responses to turbulence, its effect on the pitch rate response is secondary and it has little effect on the yaw rate response[6].

Because turbulence spatial correlations increase with the increment of flight altitude, the effect of the transverse correlations on the helicopter handling qualities in turbulent atmospheric environment with flight altitude is further discussed. A ratio between the Root-Mean-Square (RMS) value of the roll rate response with full helicopter in turbulence for the case with the unrelated filters to that with the related filters is defined for quantitative analysis,

$$\gamma_p = \frac{\sigma'_p}{\sigma_p} \times 100\% \tag{40}$$

where σ'_{p} is the RMS value of the roll rate response to turbulence for the case with the unrelated filters, and σ_{p} is the RMS value of the roll rate response to turbulence for the case with the related filters. From Eq. (40) it can be seen that the effect of the transverse correlations on the roll rate response to turbulence increases with the decrement of γ_{p}.

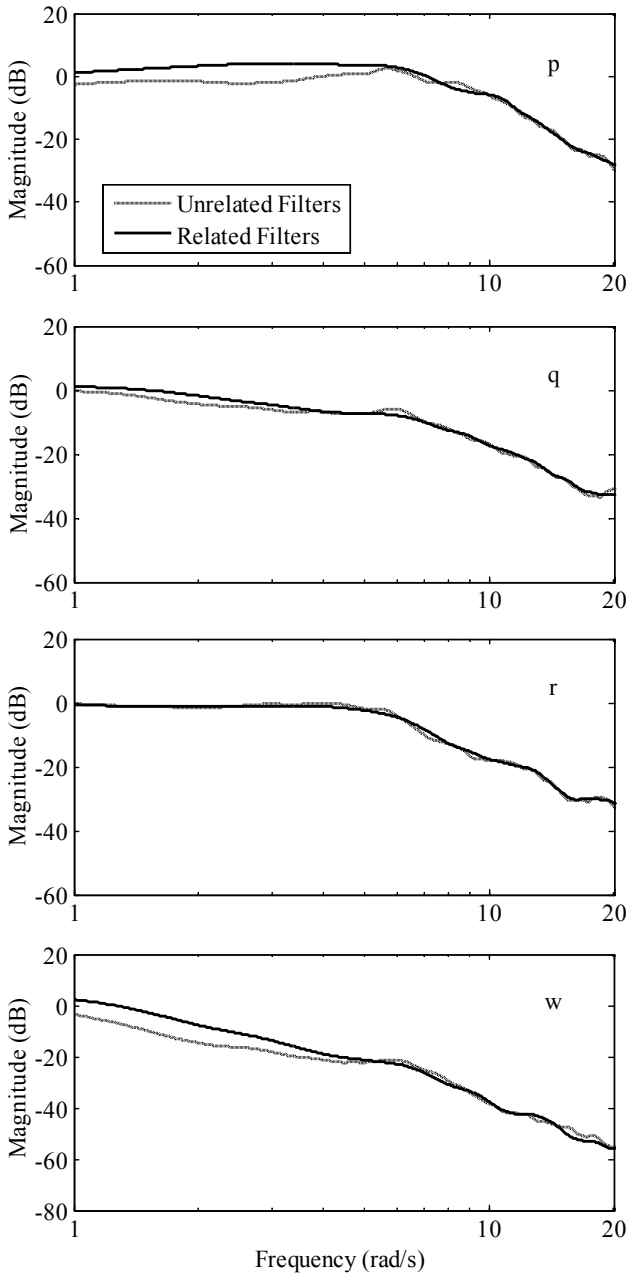

Fig. 9. Comparison of helicopter angular and heave rate responses to turbulence.

Fig. 10 shows the effect of the transverse correlations on the helicopter roll rate response to turbulence with flight altitude. The flight condition is the same as above. It can be found that neglect of turbulence transverse correlations would result an underestimate of roll rate response to atmospheric turbulence by about 25% for the flight condition with low flight altitude, and the underestimate increases with the flight altitude and is up to about 40% at the altitude of 300 m. This is because for the turbulence model with the related filters, the transverse correlations of the turbulence disturbances over the main rotor increase with the increment of flight altitude, which results in the reduction of the "rotor-to-body attenuation" effect, while for the model with the unrelated filters the transverse correlations of the turbulence disturbances over the main rotor don't vary with flight altitude.

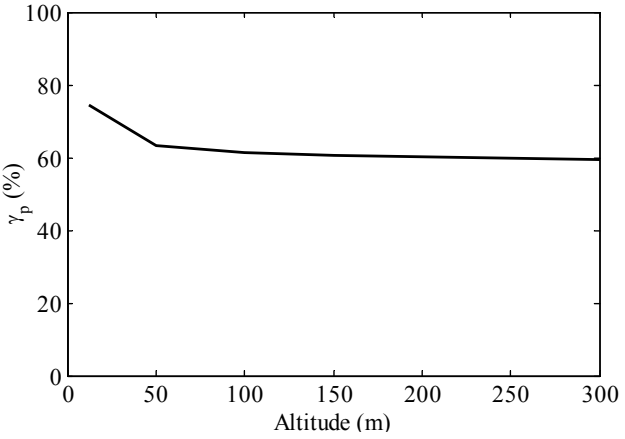

Fig. 10. Effect of turbulence transverse correlations on helicopter roll rate response with flight altitude.

5. CONCLUSIONS

This paper developed a distributed turbulence model with the von Karman correlations for helicopter flight simulation and handling-quality analysis. The effects of turbulence longitudinal and transverse correlations on the helicopter handling qualities in turbulent atmospheric environment were discussed with the frequency responses of heave and angular rates. The following conclusions can be gotten:

(1) The spectra and correlation coefficients of the turbulence velocity components by the distributed model show an excellent agreement with those of the theoretical von Karman model. It is suggested that the Nyquist frequency of the sampling period for the helicopter handling-quality analysis in atmospheric turbulence should be larger than three times of the interested frequency.

(2) Analysis of helicopter handling qualities in turbulent atmospheric environment by the turbulence models based on the Dryden and von Karman filters results in different results. The difference increases

with the increment of flight altitude and the decrement of airspeed. The proposed turbulence filters based on the longitudinal correlations of the von Karman model improves the accuracy of helicopter handing-quality analysis in the higher interested frequency for the flight conditions with low airspeed and high altitude.

(3) Turbulence transverse correlations have important impact on the helicopter handling qualities of both the roll and heave axes in the lower interested frequency range, have a little impact on that of pitch axis, but nearly have no effect on that of yaw axis. The proposed turbulence model with transverse correlations improves the accuracy of helicopter handling-quality analysis in the lower frequency range.

ACKNOWLEDGMENTS

This work was supported by the National Natural Science Foundation of China (Grant Number: 11672128).

REFERENCES

[1] ANON. MIL-F-8785C, Flying Qualities of Piloted Airplanes[S]. Washington: U.S. Department of Defense, 1980.

[2] DANG Y Y, GAONKAR G H, PRASAD J V R. Parallel Methods for Turbulence Simulation and Helicopter Response Prediction[J]. Journal of the American Helicopter Society, 1996, 41(3): 219-231.

[3] VAN GOOL P C A. Rotorcraft Responses to Atmospheric Turbulence[D]. Delft, The Netherlands: Technische Unversiteit Delft, 1997.

[4] GAONKAR, G. H. Review of Turbulence Modeling and Related Applications to Some Problems of Helicopter Flight Dynamics[J]. Journal of the American Helicopter Society, 2008, 53(1): 87-107.

[5] MCFARLAND R E, DUISENBERG K. Simulation of Rotor Blade Element Turbulence, NASA TM-108862[R]. Washington: NASA 1995.

[6] JI H L, CHEN R L, LI, P. Distributed Atmospheric Turbulence Model for Helicopter Flight Simulation and Handling Quality Analysis[J]. 2017, Journal of Aircraft, 54(1): 190-198.

[7] LABOWS S J. UH-60 Black Hawk Disturbance Rejection Study for Hover/Low Speed Handling Qualities Criteria and Turbulence Modeling[D]. Monterey, CA: Naval postgraduate school, 2000.

[8] LUSARDI J A, BLANKEN C L, TISCHLER M B. Piloted Evaluation of a UH-60 Mixer Equivalent Turbulence Simulation Model[C]//Proceedings of 59th Annual Forum of American Helicopter Society, AHS International, 2003: 309-320.

[9] SEHER-WEISS S, VON GRUENHAGEN W. Development of EC 135 Turbulence Models via System Identification[J]. Aerospace Science and Technology, 2012, 23(1): 43-52.

[10] JI H L, CHEN R L, LI P. Analysis of Helicopter Handling Quality in Turbulence with Recursive Von Kármán Model[J]. Journal of Aircraft, in print, 2017.

[11] KATZ P. Digital Control Using Microprocessors. Prentice-Hall International, INC, USA. 1981: 47-64.

[12] ETKIN B. Dynamics of Atmospheric Flight. John Wiley and Sons, Inc., New York, USA. 1972: Chapter 13.

[13] ASCHER U M, CHEN G. A First Course in Numerical Methods. Society for Industrial and Applied Mathematics, Philadelphia, USA. 2011: 104-107.

[14] HOWLETT J J. UH-60A Black Hawk Engineering Simulation Program, NASA CR- 166309[R]. Washington: NASA, 1981.

[15] LI P, CHEN R L. A Mathematical Model for Helicopter Comprehensive Analysis[J]. Chinese Journal of Aeronautics, 2010, 23(3): 320-326.

[16] MCRUER D T, JEX H R. A Review of Quasi-Linear Pilot Models[J]. IEEE Transactions on Human Factors in Electronics, 1967, 8(3): 231-249.

[17] BALLIN M G, DALANG-SECRÉTAN M A. Validation of the Dynamic Response of a Blade-Element UH-60 Simulation Model in Hovering Flight[J]. Journal of the American Helicopter Society, 1990, 36(4): 77-88.

[18] KIM F D, CELI R, TISCHLER M B. Forward Flight Trim Calculation and Frequency

Response Validation of a High-Order Helicopter Simulation Model[J]. Journal of Aircraft, 1993, 30(6): 854-863.

[19] SMITH R H. A Theory for Handling Qualities with Applications to MIL-F-8785B, AFFDL-TR- 75-119[R]. Air Force Flight Dynamics Laboratory, Wright-Patterson AFB, OH, Oct. 1976.